Muhammad Azam ✉
Mirza Jahanzaib

https://doi.org/10.21278/TOF.494072024
ISSN 1333-1124
eISSN 1849-1391

OPTIMISATION OF CUTTING PARAMETERS USING AN EMPIRICAL MODEL TO ACHIEVE THE APPROPRIATE SURFACE ROUGHNESS OF AN O-RING GROOVE

Summary

This study was conducted to investigate the effects of cutting parameters (cutting speed, feed rate, and depth of cut) on the average roughness (R_a) of an O-ring groove base by performing grooving experiments on titanium alloy (Ti6Al4V) using coated carbide tools and oil-based coolant. The experimental design is based on a central composite design template of response surface methodology. The results show that the relationship between the cutting parameters and average roughness is best represented by a quadratic model. ANOVA was employed to check the adequacy of the proposed model and the percentage contribution of significant factors to the development of the model. Feed was the most significant factor, with the largest contribution of 67.05%, followed by the quadratic and interaction terms. The results of the additional validation runs showed that the predicted roughness matched reasonably well the actual roughness, with an average prediction error of 15.8%. The contour plots and response surfaces developed in this study will help in selecting the optimum machine parameters for the desired roughness of the O-ring groove base.

Key words: *surface roughness; O-ring groove; titanium alloy; empirical model; coated carbide tool*

1. Introduction

Mechanical parts used in the aerospace and automobile industries require a high surface finish. Various functional properties, such as fatigue strength, corrosion and wear resistance, and the formation and rupture of oil film at the rod seal interface, depend on the final average roughness. The optimised surface texture of a cylinder bore contributes to increased engine performance and durability [1-3].

Factors that affect the surface finish of machined parts include tool type, the sharpness of the cutting edges, the width of the grooving insert, tool overhang, cutting parameters, cutting fluid, a shank vs dampened cutting tool, nose radius, etc. [4]. Research focusing on the effect of these parameters on the roughness average are studied and elaborated in the literature review. Little research work has been conducted to optimise the cutting parameters for the surface roughness of an O-ring groove base.

The present study aims to investigate the relationship between the cutting parameters and the roughness of the O-ring groove base, develop an empirical model, and optimise the cutting parameters for the desired range of average roughness by employing response surface methodology (RSM). The contribution to research is to optimise R_a for the desired roughness average of the O-ring groove base by employing titanium alloy (Ti6Al4V) under an annealed condition. Grooving operations are generally performed at the final assembly stage; therefore, meeting the required quality parameters/characteristics is vital. The remainder of this paper is organised as follows. Section 2 presents the research conducted in the areas of tool parameters, cutting fluid, machine parameters, and statistical design. Section 3 elaborates the experimental details, including the machine tool, workpiece composition and properties, cutting conditions, and cutting tool parameters. Section 4 outlines the experimental methodology, response data, and the statistical and residual analyses. Conclusions based on plots of significant effects, contour plots, and 3D response surfaces are presented in Section 5, along with the data validation results. Finally, Section 6 presents the conclusions drawn from this study.

2. Literature review

Surface roughness is essentially the machining marks left on a surface by the tool/process used to produce it. It cannot be completely eliminated due to practical constraints, such as the limitation of the processing equipment [1]. The final value of the surface roughness depends on numerous factors such as the tool parameters, the type of cutting fluid used, and the cutting parameters. This section presents previous research related to the effects of these parameters on the surface roughness.

Tool parameters include tool geometry, the type of coatings, and tool materials. Shokrani and Newman [5] studied the effect of tool geometry (rake angle and clearance angle) on tool wear and surface roughness. Titanium alloy, Ti6Al4V, was machined in a cryogenic environment using a cemented tungsten carbide cutting tool. The study showed that tool life and mean surface roughness improved when the rake angle was changed from 10° to 14°. A change in the primary clearance angle from 8° to 10° resulted in almost same R_a value when inserts with a rake angle of 14° were used. Li et al. [6] used uncoated carbide inserts to optimise the cutting parameters for surface roughness, the material removal rate, and specific cutting energy. A quadratic model was proposed for each response based on the experimental data. Sun et al. [7] investigated the effect of cutting parameters on tool temperature and cutting forces while milling titanium alloy (Ti6Al4V). Cemented carbide tools were used to perform the experiments. The cutting temperature and cutting forces were found to increase with an increase in cutting speed and feed, while an increase in the depth of cut did not result in any significant increase in the temperature. Korkut et al. [8] performed turning experiments using multilayer coated cemented carbide tools. They established how tool wear/surface roughness were correlated with the chip produced at three different cutting speeds.

The type of cutting fluid used also influences the final surface roughness. Liew et al. [9] investigated the effect of the machine parameters on tool wear and surface roughness using carbon nanofiber nano fluid and deionized water as coolants. Experiments were performed using the PVD-coated carbide insert DNMG 150408N. Speed was found to be the most important parameter affecting tool wear while feed was a dominant factor in controlling R_a. Sneddon et al. [10] investigated the relationship between the surface roughness and failure response of two key aerospace titanium alloys, Ti64 and Ti407. Polished, grounded, and sandblasted specimen surfaces were prepared. The results showed that magnitude as well as the orientation of the surface roughness for Ti6Al4V parts were significant and must be accounted for during the design phase. However, Ti407 was insensitive to surface roughness due to its relatively greater ductility.

Besides tool parameters and cutting fluid, cutting parameters (speed, feed, and depth of cut) play a major role in controlling the surface finish of machined parts. Bouzid et al. [11] used multilayer coated carbide tools (SNMG 120408-MF) to study the effect of machine parameters on tool wear, surface roughness, and tool life. A desirability function approach was used to optimise multiple responses. The average prediction errors for tool wear, the average surface roughness, and tool life were reported to be 6.38%, 4.44% and 3.76%, respectively. Trabelsi et al. [12] compared the effects of cutting parameters on tool life and cutting forces when titanium alloy Ti17 was turned using a shank tool (PCLNR 2525M12) fitted with a CNMG 120412-23 H13A insert under conventional lubrication and cryogenic conditions (liquid nitrogen). A significant improvement in tool life was noticed under cryogenic cooling. The extent of the improvement depended on the cutting parameters used. However, little improvement was observed in the cutting forces. Azam et al. [13] employed RSM to study the effects of the cutting parameters on the surface roughness of high strength low alloy (HSLA) steel. The linear model best described the relationship between the response and input parameters. Feed was found to be the most influential factor. Peng et al. [14] compared high speed ultrasonic vibration cutting (HUVC) with the conventional cutting (CC) of titanium alloy (Ti6Al4V) in terms of machinability, wear resistance, surface roughness, microstructure, and residual stresses. The results showed that in comparison with CC, HUVC resulted in the improved wear resistance of titanium alloy (Ti6Al4V) and reduced surface roughness.

A precise experimental design methodology is essential to study the relationship of machine parameters and the roughness parameter (R_a). Benardos and Vosniakos [15] classified different approaches used by researchers to predict surface roughness based on the theory of machines, artificial intelligence (AI), and the design of experiments. RSM and the Taguchi technique for the design of experiments (DoE) are reported to be the most commonly used methodologies for predicting surface roughness. Seikh et al. [16] performed end milling experiments on oxygen-free high conductivity copper (OFHC) to study the effect of cutting parameters on R_a and R_z. The central composite design (CCD) of RSM methodology was used to design the experimental runs. It was concluded that the radial depth of cut had the greatest influence on the average surface roughness. Abbasi et al. [17] used the Taguchi technique (L_{18} orthogonal array) to analyse the effects of cutting speed, feed, and three titanium alloys on cutting tool temperature, cutting force, and feed force. The results showed that the feed rate had the most significant impact on both force components. The cutting tool temperature was mostly affected by speed.

From the literature review, it is clear that the cutting tools, cutting fluid, and cutting parameters significantly affect the roughness parameters of the machined surface. It is also evident that cutting parameters impact the final surface roughness when the operation changes from single-point cutting (turning) to multiple-point cutting (milling) to forming operations (grooving). However, little effort has been made to evaluate the effect of cutting parameters on the surface roughness of an O-ring groove base. O-rings (Fig. 1) are used in many critical applications, including subsea hydraulic systems and hydrogen storage systems to prevent fluid leakage. They must be reliable and stable to successfully perform subsea tasks and prevent the detrimental effects of seawater intrusion. It is therefore imperative to know the materials and factors that contribute to fluid leakage at low temperatures and in high pressure applications [18-19].

Engineering documents and the literature specify certain limits on the average roughness of the O-ring groove base. For static seals intended for liquid applications, the O-ring groove base should have an average roughness in the range of 32-63 μin (0.8-1.6 μm). For gaseous applications, the roughness should lie between 16 and 32 μin (0.4-0.8 μm). For dynamic applications where relative motion exists between the O-ring and one or more parts, the maximum groove base roughness should be 8-16 μin (0.2-0.4 μm) for sliding contact applications and 16-32 μin for rotary contact applications. It must not be less than 5 μin [20].

Fig. 1 Basic O-ring [21]

The present research work focuses on studying the impact of cutting parameters on the surface roughness of an O-ring groove base. Grooving experiments were performed on titanium alloy (Ti6Al4V) using coated carbide tools. The central composite design (CCD) of RSM methodology was employed to design experimental runs and for the subsequent development of an empirical model with a 95% confidence interval.

3. Experimental details

This section elaborates on the machine tool, workpiece, the various tests performed on the workpiece, and the cutting conditions used during the experiments.

A titanium rod (Ti6Al4V) with a diameter of 50 mm and length of 495 mm was used to perform the grooving experiments with oil-based coolant rushing through the nozzle onto the cutting tool. Turning experiments were performed on a horizontal axis CNC lathe machine CTX 500 with a spindle power of 27 kW, maximum torque of 800 Nm, and maximum spindle speed of 4500 rpm. The width and depth of each groove were 15mm and 3mm, respectively. Grooves were machined to be slightly larger (width 15 mm) than standard grooves, keeping in mind the limitations of the available measuring equipment and to ensure repeatability and accuracy of the measurement results. Fig. 2 schematically shows the grooving operations performed on the horizontal CNC lathe.

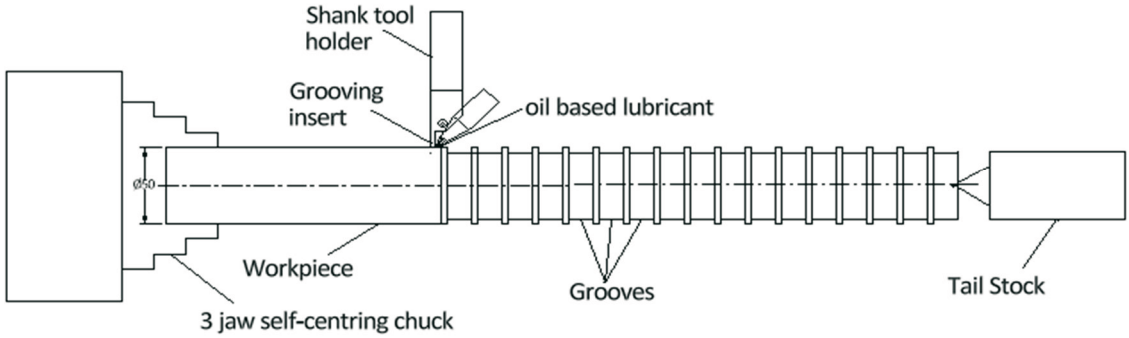

Fig. 2 Schematic representation of grooving operations on CNC lathe

Titanium alloy (Ti6Al4V) has a high strength-to-weight ratio and can withstand high temperatures. Being biocompatible, lightweight, and corrosion resistant, it has found numerous applications in the aerospace and medical industries. It is one of the most widely used titanium alloys and accounts for 50% of global production [22-24].

Machining of the titanium alloy poses a number of challenges, such as shorter tool life, poor surface integrity, and reduced production. As titanium alloys have low thermal conductivity, heat is concentrated in a small area, leading to softening of the cutting tool and chemical reaction between the tool and the workpiece [5]. Three trial tests were performed beforehand to ensure that the range of the cutting parameters chosen was appropriate and the tool can withstand cutting forces and temperature with normal wear and tear during the actual

experiments. The objective of the research study is to optimise the cutting parameters for the desired roughness of the O-ring groove base. All the experiments were performed in random order to ensure a normal and independent distribution of errors.

Experiments were performed using PVD-coated carbide inserts (N123G1-0300-0002-CM 1125) with a TiAlN layer (Fig. 3). The geometry of the insert was as follows:

insert width, l_a = 3 mm; front angle, Ψ_r = 0°; rake angle,
αf = 7°; corner radius, r_ε = 0.2 mm

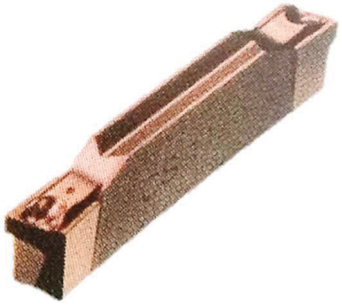

Fig. 3 Cutting insert for grooving experiments [25]

Inserts were changed after every three experimental runs to minimise the impact of tool wear in the final analysis of the surface roughness parameter (R_a).

Before conducting the experiments, the titanium bar was analysed for its composition, mechanical properties, and microstructure. Table 1 shows the workpiece composition determined through a spectrometer. Table 2 specifies the mechanical properties found after the tensile testing of the samples. The tensile samples were carefully prepared in accordance with ASTM E8M. A universal testing machine with a maximum load capacity of 250 KN was used to determine the actual mechanical properties, including ultimate tensile strength (UTS), yield strength (YS), and Young's modulus (E). The values shown were determined experimentally to ensure that the available workpiece properties lie within the range of standard values and can be used for further experimental work.

Table 1 Chemical composition of the titanium workpiece

V	Fe	Al	C	O	N	H	Balance
3.85	0.27	6.41	0.09	0.033	0.007	0.006	89.3

The cutting parameters for the experimental work were set on the basis of the mechanical properties. The mechanical properties of the work piece are shown in Table 2.

Table 2 Mechanical properties of the work piece

UTS (MPa)	**YS (MPa)**	**E (GPa)**	**% elongation**
952-963	901-907	121-122	16-17

The work piece hardness was checked using the Rockwell Hardness Tester Vexus SHR-150M with an average hardness of 31.2 HRC.

The sample was carefully prepared to obtain a flat, smooth surface for photomicrography. The microstructure of the base metal captured using a Leica microscope at a magnification of 200X is shown in Fig. 4.

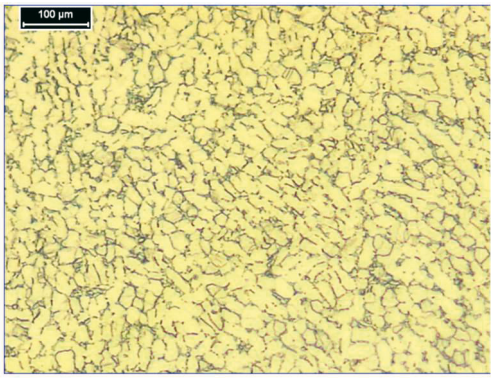

Fig. 4 A photomicrograph of α+β structure in Ti6Al4V alloy [200X]

The range of cutting parameters was carefully chosen keeping in mind the tool manufacturer's recommendations, the trial tests, and professional experience. Table 3 shows factors including speed (V), feed (f), depth of cut (d) and their levels used while performing the experiments.

Table 3 Levels of independent variables

Factors	Levels				
	Lowest	Low	Centre	High	Highest
V (m/min)	41.6	45	50	55	58.4
f (mm/rev)	0.09	0.12	0.17	0.22	0.25
d (mm)	0.5	0.6	0.75	0.9	1.0
Coding	-1.682	-1	0	1	1.682

The roughness average (R_a) was measured using a portable surface roughness tester, SURFTEST SJ-210, equipped with a deep groove detector (Fig. 5).

Fig. 5 SURFTEST SJ-210 for measuring the roughness parameter [26]

A special cylindrical attachment was designed and built to hold the drive unit on the work piece during measurements for stability and safety reasons (Fig. 6).

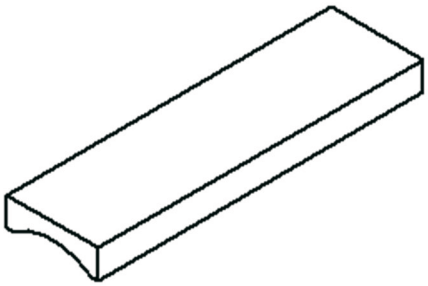

Fig. 6 Cylindrical attachment for safe and reliable roughness measurements

4. Experimental design

Response surface methodology was employed to optimise average roughness (R_a). RSM is a collection of mathematical and statistical techniques used to model and analyse problems in which response depends on a number of factors and where the objective is to optimise the response [27]. The model was developed by employing the design of experiments approach in combination with regression techniques.

Design expert 13 was used to design and analyse the experimental data.

4.1 Central composite design

Typical designs used for RSM include central composite design (CCD), Box Behnken design (BBD), and computer-generated optimal designs [28]. In this study, all the experimental runs were based on rotatable central composite design (CCD). Replication runs (centre points) were added to help estimate pure error. The complete design matrix, along with the response data, is shown in Table 4. All the experiments were performed in random order to ensure that the errors are distributed normally and independently.

4.2 Statistical analysis

Table 4 shows that the values of R_a lie in the range of 0.293-1.467 µm. Table 5 shows the model summary statistics for R_a. Since it is evident from the table that the quadratic model is the best suggested model for the average roughness, it was used for further analysis.

Table 4 CCD design matrix with actual and coded factors and response measurements

Std	Run	V (m/min)	f (mm/rev)	d (mm)	Coding			R_a (µm)
					X1	X2	X3	
1	14	45.00	0.12	0.60	-1.000	-1.000	-1.000	0.293
2	7	55.00	0.12	0.60	1.000	-1.000	-1.000	0.417
3	12	45.00	0.22	0.60	-1.000	1.000	-1.000	0.914
4	8	55.00	0.22	0.60	1.000	1.000	-1.000	1.029
5	3	45.00	0.12	0.90	-1.000	-1.000	1.000	0.563
6	13	55.00	0.12	0.90	1.000	-1.000	1.000	0.405
7	16	45.00	0.22	0.90	-1.000	1.000	1.000	0.984
8	15	55.00	0.22	0.90	1.000	1.000	1.000	0.706
9	10	41.59	0.17	0.75	-1.682	0.000	0.000	0.705
10	2	58.41	0.17	0.75	1.682	0.000	0.000	0.614
11	5	50.00	0.09	0.75	0.000	-1.682	0.000	0.601
12	18	50.00	0.25	0.75	0.000	1.682	0.000	1.467
13	1	50.00	0.17	0.50	0.000	0.000	-1.682	0.459
14	4	50.00	0.17	1.00	0.000	0.000	1.682	0.706
15	6	50.00	0.17	0.75	0.000	0.000	0.000	0.708

Std	Run	V (m/min)	f (mm/rev)	d (mm)	Coding			R_a (μm)
					X1	X2	X3	
16	9	50.00	0.17	0.75	0.000	0.000	0.000	0.702
17	11	50.00	0.17	0.75	0.000	0.000	0.000	0.682
18	19	50.00	0.17	0.75	0.000	0.000	0.000	0.565
19	17	50.00	0.17	0.75	0.000	0.000	0.000	0.767

Table 5 Model summary statistics for R_a data

Source	Std. Dev.	R^2	Adjusted R^2	Predicted R^2	PRESS	
Linear	0.1630	0.6867	0.6240	0.4355	0.7181	
2FI	0.1600	0.7586	0.6379	0.4783	0.6636	
Quadratic	0.0902	0.9424	0.8848	0.6657	0.4252	Suggested
Cubic	0.1034	0.9580	0.8487	-4.4986	6.99	Aliased

4.3 Quadratic model

The non-linear relationship between the cutting parameters and average roughness (Ra) in terms of actual factors is given by

$$R_a = -9.17969 + 0.210976 * A + 0.697056 * B + 11.0981 * C - 0.0645 * AB - 0.1125 * AC - 8.49444 * BC - 0.00120772 * A\text{^}2 + 40.8615 * B\text{^}2 - 2.54923 * C\text{^}2$$

Table 6 shows ANOVA for the average roughness. The model F value of 16.37 reveals that the model is significant. Feed (f) and interaction between speed and depth of cut (AC) and the quadratic terms B^2 and C^2 are significant model terms as their p-values are less than 0.05. The replicates in the design helped determine the statistics such as lack of fit and pure error. Table 7 compares the F ratio for lack of fit to the standard F ratio at a 95% confidence level by taking into account degrees of freedom for lack of fit and pure error. The model F value for lack of fit (1.88) is smaller than the standard value ($F_{0.05,\,5,\,4}$ =6.256), indicating that lack of fit is NOT significant relative to pure error, and that the model is adequate. Table 6 also shows the value of R^2 and adjusted R^2 is 0.942 and 0.884, respectively. Adequate precision measures the signal-to-noise ratio. Its value must not be less than 4. Adequate precision for the average roughness (R_a) model is 17.01, which indicates an adequate signal. Hence, the model can be used to navigate the design space.

Table 6 Analysis of variance for average roughness R_a (μm)

Source	Sum of squares	df	Mean square	F-value	p-value	Contribution. %	
Model	1.20	9	0.1332	16.37	0.0001		*significant*
A-V	0.0090	1	0.0090	1.11	0.3202	0.71	
B-f	0.8516	1	0.8516	104.64	0.0001	67.05	*significant*
C-d	0.0129	1	0.0129	1.59	0.2391	1.02	
AB	0.0021	1	0.0021	0.2556	0.6253	0.16	
AC	0.0570	1	0.0570	7.00	0.0267	4.49	*significant*
BC	0.0325	1	0.0325	3.99	0.0769	2.56	
A^2	0.0124	1	0.0124	1.53	0.2475	0.98	
B^2	0.1424	1	0.1424	17.50	0.0024	11.21	*significant*
C^2	0.0449	1	0.0449	5.52	0.0434	3.54	*significant*
Residual	0.0732	9	0.0081				
Lack of fit	0.0514	5	0.0103	1.88	0.2807		*NOT significant*

Source	Sum of squares	df	Mean square	F-value	p-value	Contribution. %
Pure error	0.0219	4	0.0055			
Cor. total	1.27	18				
Std. dev.			0.0902		R^2	0.9424
Mean			0.6993		Adjusted R^2	0.8848
C.V. %			12.90		Adeq. precision	17.0109

Table 7 Results of model adequacy analysis

Response	Degree of freedom		F value		Model status
	LOF	Pure error	Model	Standard	
R_a	5	4	1.88	6.256	*Adequate*

4.4 Residual analysis

Residual analysis is a primary tool used to check the model adequacy and the assumptions underlying ANOVA. It is assumed that the residuals are normally distributed, independent, and have constant variance. The recommended plot to check these assumptions is the "normal plot of residuals" [27]. Fig. 7 shows the normal plot of residuals for average roughness (R_a). All data points lie along a straight line, indicating that the underlying errors are normally and independently distributed.

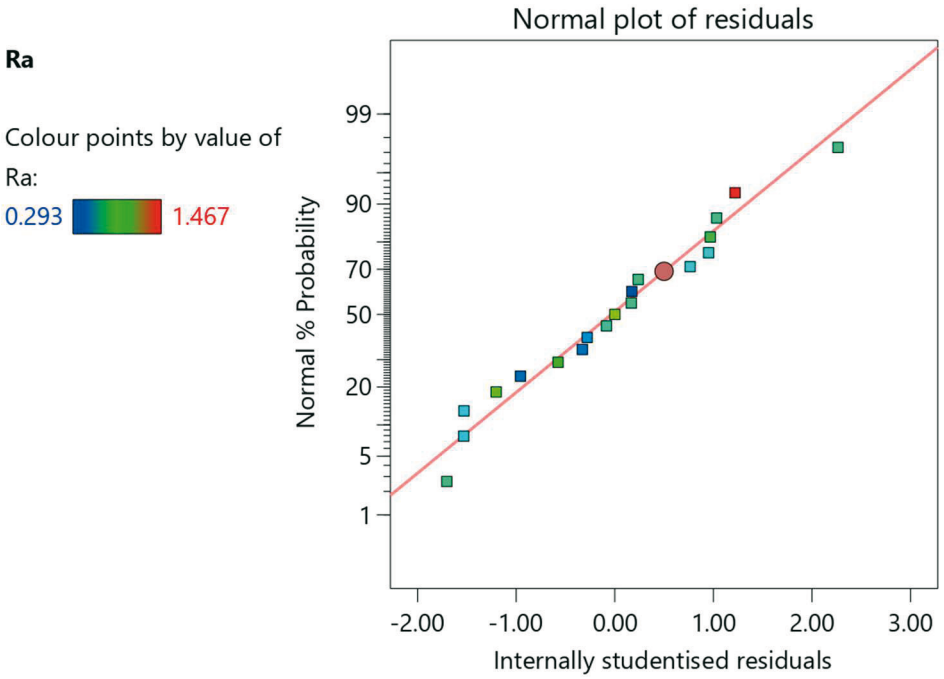

Fig. 7 Normal plot of residuals for R_a data

Fig 8 shows the plot of residuals in the time sequence of the experimental runs. The graph does not show any tendency of positive or negative residuals. Instead, it shows a random scatter which indicates that the errors are normally distributed and no lurking time-related variable influenced the response during the experiments. Fig. 9 shows the plot of actual vs predicted values for R_a data points. All the data points are evenly distributed about the 45-degree line.

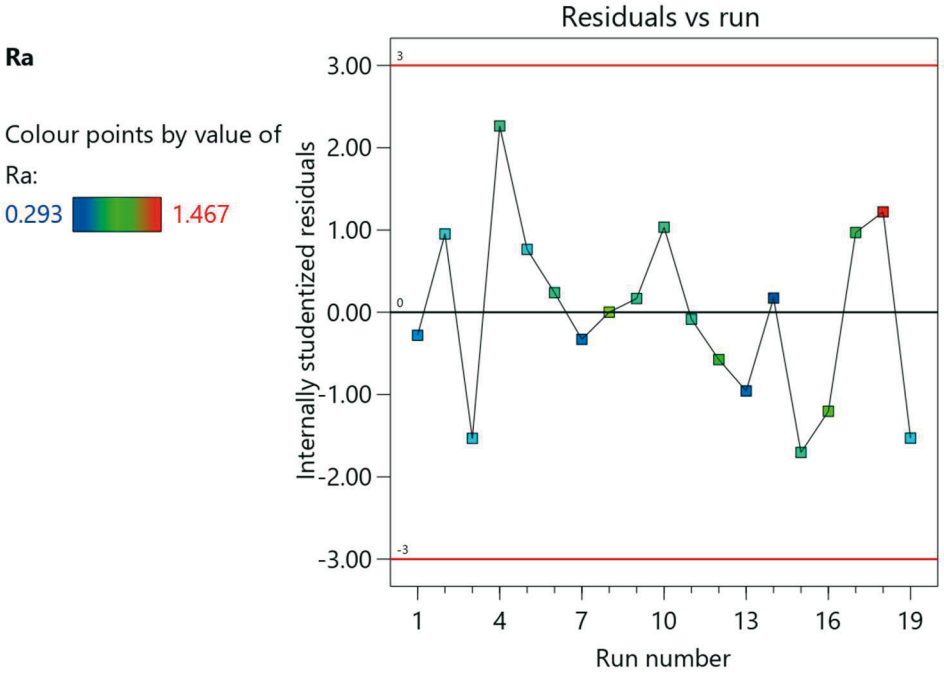

Fig. 8 Plot of residuals vs run number for R_a

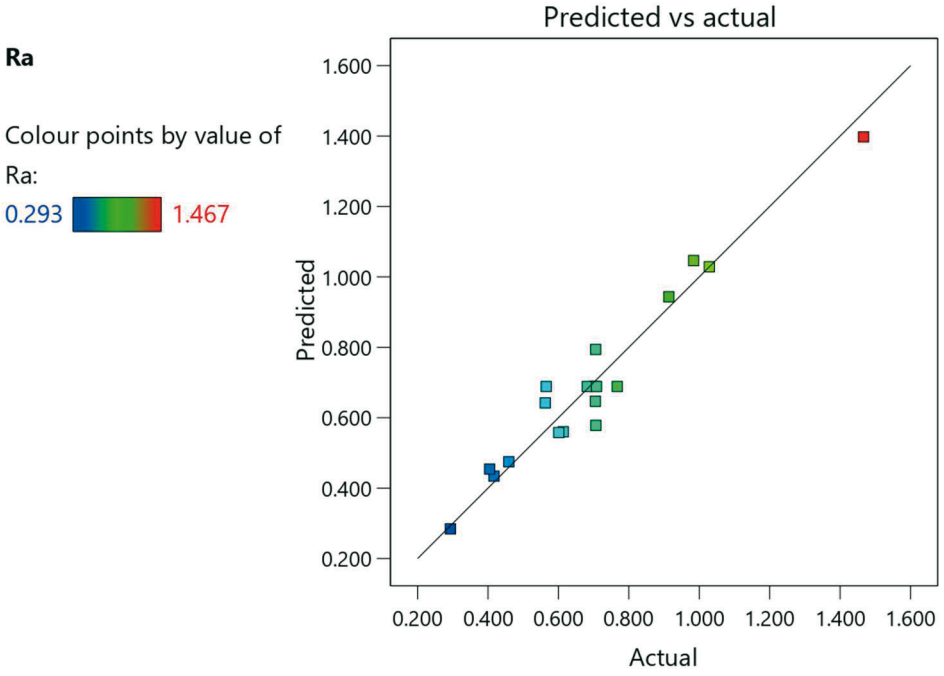

Fig. 9 Plot of predicted vs actual values for R_a

5. Results and discussion

5.1 Interaction effects

Table 6 shows the percentage contribution of all the factors to the average roughness of the O-ring groove base. From the table, it is clear that feed significantly affects the R_a with a contribution of 67% towards the model development. An increase in feed leads to a rise of average roughness of the groove base. The quadratic term (B^2) is the next dominant factor with a contribution of 11.2%, followed by interaction between cutting speed and depth of cut and the factor (C^2). All remaining factors are statistically insignificant.

The main effects of speed, feed, and depth of cut on the average roughness of the groove base are not displayed here because all three factors are involved in multiple interactions. Fig 10 shows the interaction effects of (a) *V* and *f*, (b) *V* and *d*, and (c) *f* and *d*. Interaction between speed and feed is insignificant, as indicated by the overlapping LSD bars on the plot. Besides, the lines are parallel, which is an indication of insignificant interaction. The plot of the cutting speed and depth of cut interaction shows that the interaction is significant. Table 6 indicates that the p-value for the interaction effect between feed and depth of cut (BC) is slightly higher than the threshold (p value≤ 0.05) set by the 95% confidence interval. The factor is marginally significant. Fig 10(c) shows the plot of the feed and depth of cut interaction.

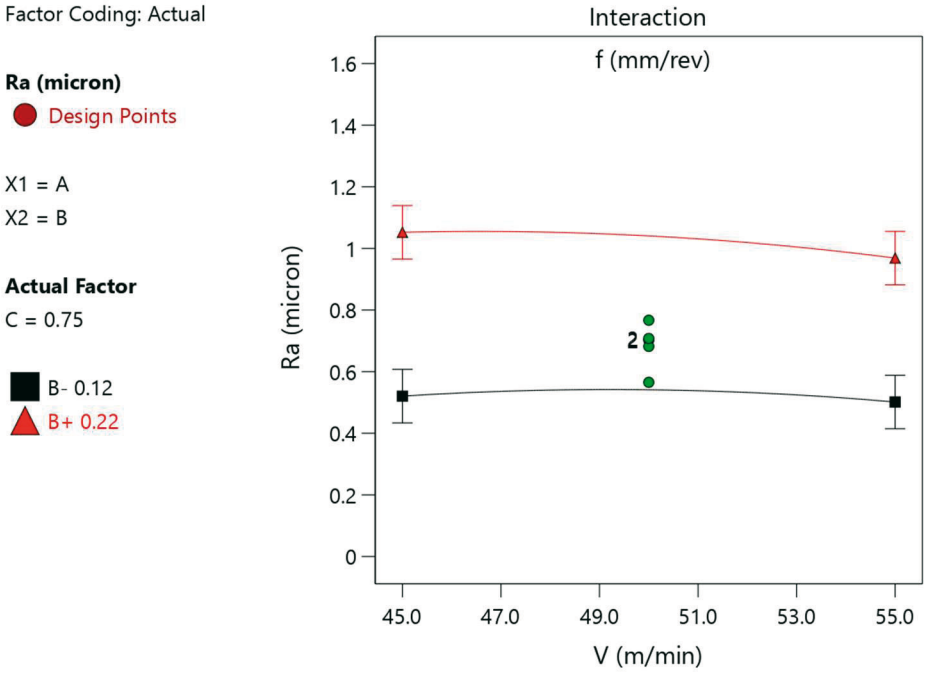

a) Speed vs feed interaction

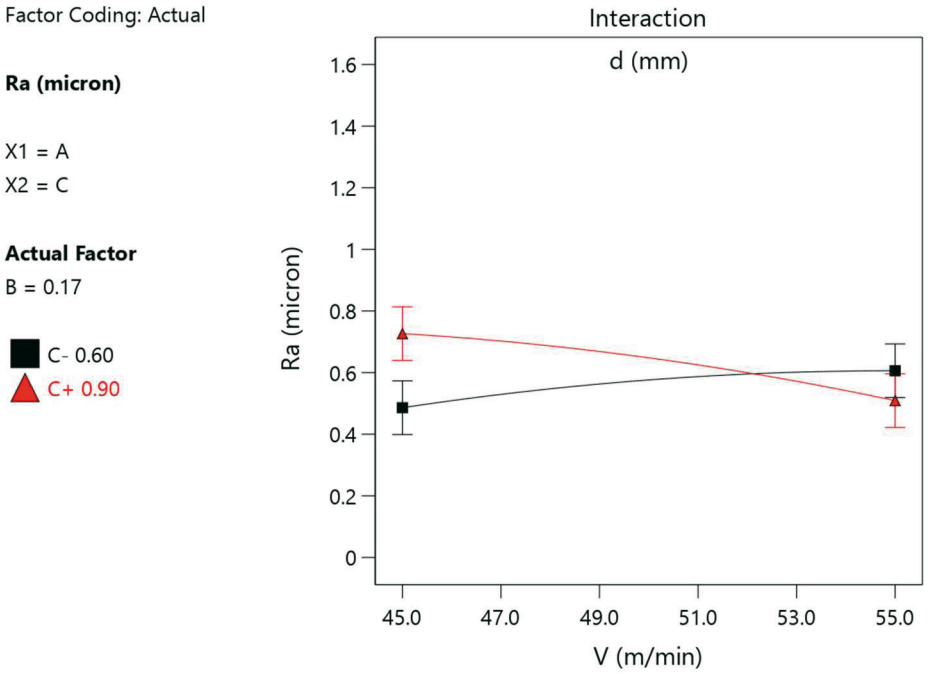

b) Speed vs depth of cut interaction

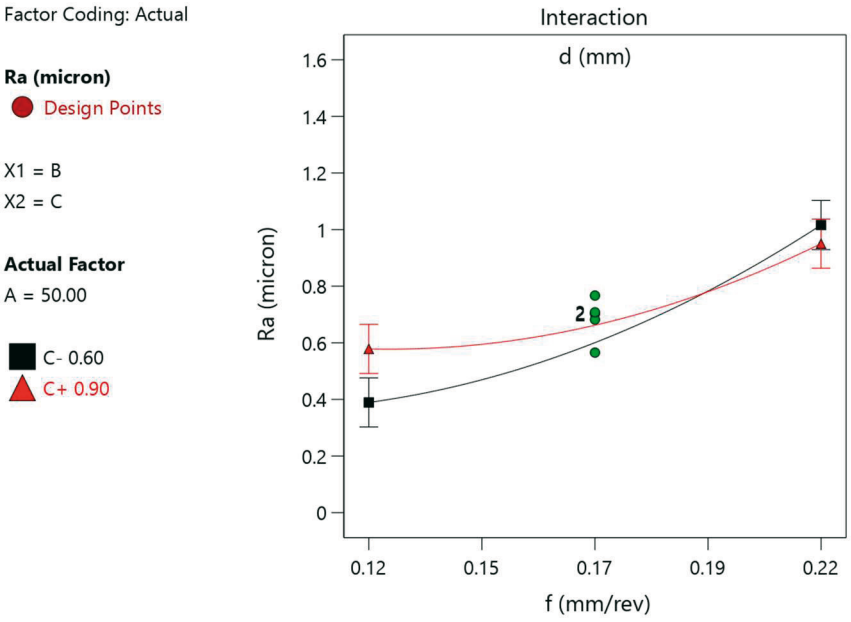

c) Feed vs depth of cut interaction

Fig. 10 Interaction effects for R_a a) V vs f, b) V vs d, c) f vs d

5.2 Contour plots and 3D response surfaces

In this section, contour plots and response surface plots are used to manipulate the empirical model. The lines of the constant response are drawn on the x–y plane in the contour plots (Fig. 11). The curved lines of constant response indicate that the interaction and quadratic terms are significant. For a given depth of cut, increasing the speed reduces the average roughness (Fig 11b). The contour plots help predict the R_a value for a set of input variables. Such a prediction is shown on the contour plot using a flag. From the contour plots, we can easily set the input machine parameters (speed, feed, and depth of cut) to achieve an average roughness of the O-ring groove base in the range of 0.4-0.8 µm. Similarly, these contour plots also help decide which settings of the machine parameters will result in an R_a value below 0.4 µm. Fig. 12 shows the 3D response surfaces of the interaction effects. The planes of the response surfaces are twisted due to significant interaction and the quadratic terms, as shown in ANOVA (Table 6).

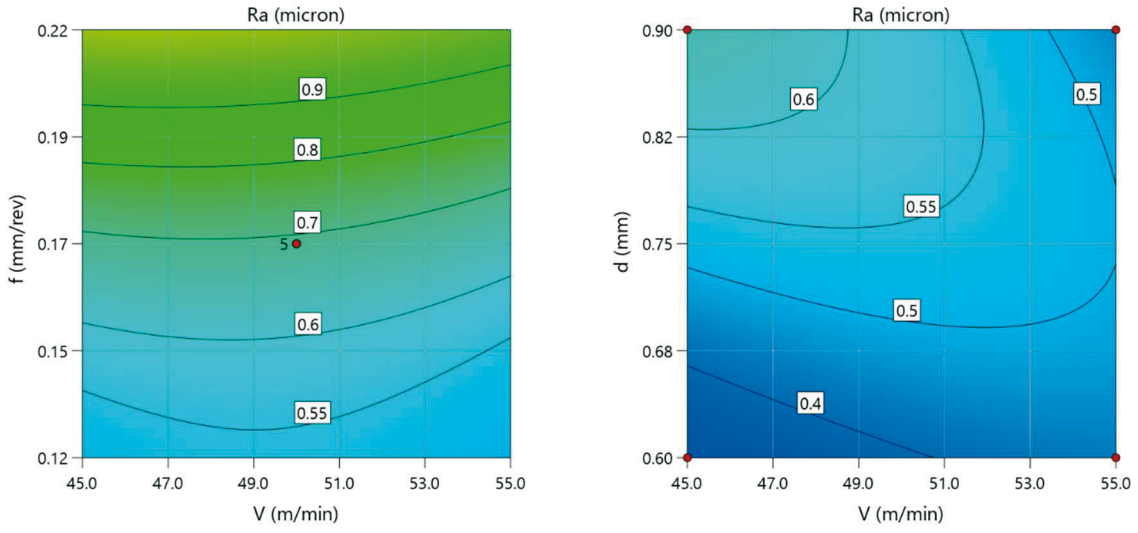

a) R_a vs speed and feed

b) R_a vs speed and depth of cut

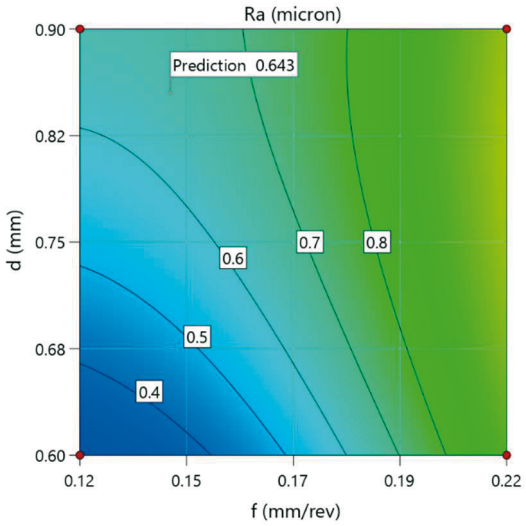

c) R_a vs feed and depth of cut

Fig. 11 Interaction contour plots a) R_a vs V and f b) R_a vs V and f c) R_a vs f and d

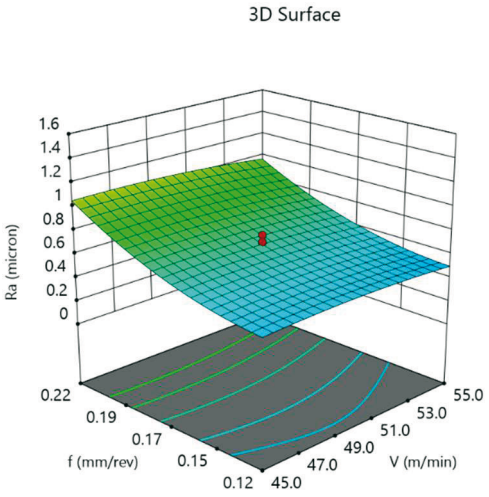

a) 3D response surface, R_a vs V and f

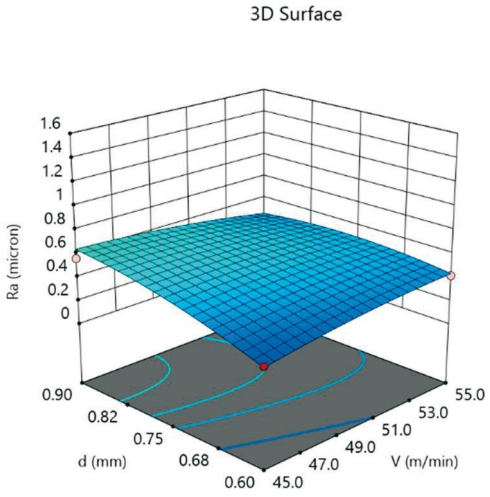

b) 3D response surface, R_a vs V and d

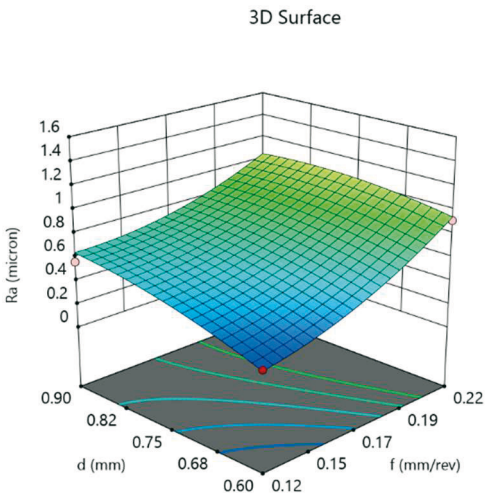

c) 3D response surface, R_a vs f and d

Fig. 12 3D response surfaces for R_a vs grooving parameters

5.3 Validation of results

From a statistical analysis carried out for R_a, it is now clear that the quadratic model adequately relates the cutting parameters with the response data. Validation of the proposed model was checked using actual data. According to Suresh et al. [29], the prediction accuracy of the RSM-based model can be found by the following relationship:

$$\Delta = \frac{100}{N} \sum_{i=1}^{N} \left| \frac{y_{i,exp} - y_{i,pred}}{y_{i,pred}} \right|$$

where Δ = percent prediction accuracy of the model; N= No. of validation runs; yi,exp= measured response value corresponding to the ith experiment; $yi, pred$= predicted response value corresponding to the ith experiment. Four additional experiments were performed for model validation purposes. Table 8 shows the actual and predicted values for *Ra*. Experimental and predicted values for *Ra* are also shown graphically in Fig. 13. The average prediction error for *Ra* for validation data is 15.8%.

Table 8 Validation data

Trial No.	M/C parameters			Predicted	Actual	Residual
	V (m/min)	f (mm/rev)	d (mm)	R_a (µm)	R_a (µm)	R_a (µm)
1	47	0.14	0.64	0.456	0.391	0.065
2	53	0.14	0.64	0.511	0.442	0.069
3	47	0.2	0.64	0.823	0.751	0.072
4	53	0.2	0.84	0.788	1.005	-0.217

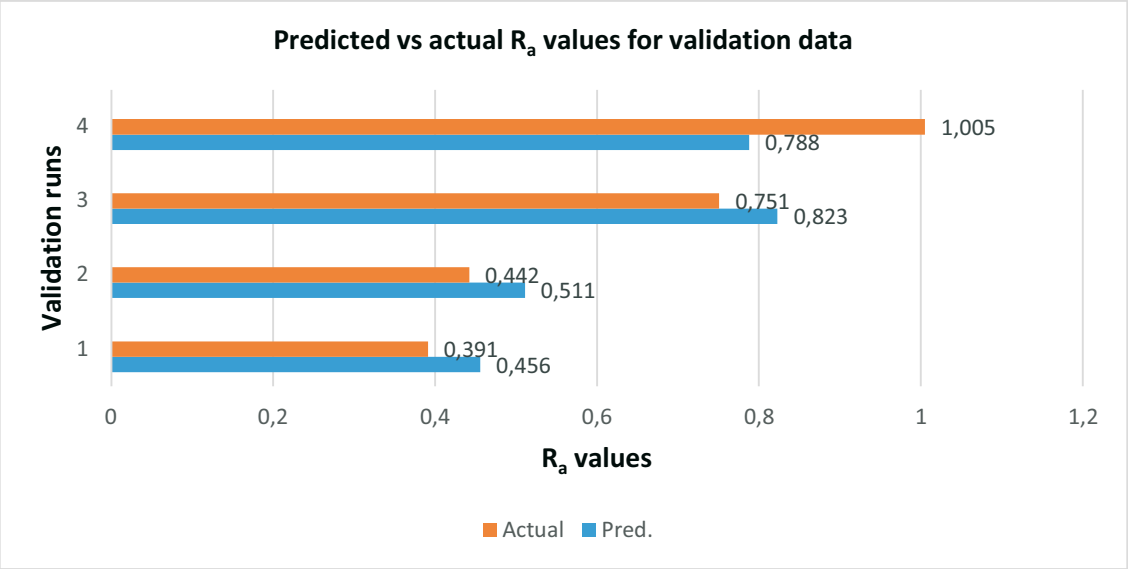

Fig. 13 Plot of predicted vs actual R_a values for validation data

6. Conclusions

This study adopted a systematic approach to evaluate the effects of speed, feed, and depth of cut on the average roughness (R_a) of an O-ring groove base of titanium alloy (Ti6Al4V) using coated carbide tools and oil-based coolant. The following conclusions are drawn from this study:

1. A surface roughness analysis was successfully performed using the CCD tool of RSM methodology. It was concluded that the design was balanced and more efficient than the OFAT experimental approach, leading to statistically independent results.

2. The quadratic model best approximated the relationship between the machine parameters and the roughness component (R_a). The lack of fit was found to be insignificant for this model.
3. ANOVA showed that feed was the most significant factor affecting the average roughness of the O-ring groove base, with a contribution of 67.05%. The quadratic factor (B^2) was the 2nd largest factor with a contribution of 11.21%, followed by the interaction between speed and depth of cut (V x d) and the quadratic term (C^2).
4. ANOVA showed that feed is the single most important factor influencing the surface roughness of the O-ring groove. For a given speed, increasing the feed results in a rougher groove surface. This can be due to higher plastic deformation and the chip formation rate.
5. An analysis of the results of the validation runs showed that predicted roughness matched reasonably well with the actual roughness with an average prediction error of 15.8%.
6. The contour plots and response surfaces will help choose the optimum cutting parameters for the desired roughness of the O-ring groove base, such as that required for gaseous applications (0.4-0.8 μm).

REFERENCES

[1] Wang, B., Meng, X., Peng, X., & Chen, Y. (2021). Experimental investigations on the effect of rod surface roughness on lubrication characteristics of a hydraulic O-ring seal. *Tribology International*, *156*, 106791. https://doi.org/10.1016/j.triboint.2020.106791

[2] La Monaca, A., Murray, J. W., Liao, Z., Speidel, A., Robles-Linares, J. A., Axinte, D. A., ... & Clare, A. T. (2021). Surface integrity in metal machining-Part II: Functional performance. *International Journal of Machine Tools and Manufacture*, *164*, 103718. https://doi.org/10.1016/j.ijmachtools.2021.103718

[3] Mezghani, S., Demirci, I., Zahouani, H., & El Mansori, M. (2012). The effect of groove texture patterns on piston-ring pack friction. *Precision Engineering*, *36*(2), 210-217. https://doi.org/10.1016/j.precisioneng.2011.09.008

[4] Coromant, S. (2010). Metal cutting technology-Technical guide. *SandvikCoromant, Sweden*.

[5] Shokrani, A., & Newman, S. T. (2019). A new cutting tool design for cryogenic machining of Ti6Al4V titanium alloy. *Materials*, *12*(3), 477. https://doi.org/10.3390/ma12030477

[6] Li, X., Liu, Z., & Liu, Z. (2019). Tool Wear, Surface Topography, and Multi-Objective Optimization ofCutting Parameters during Machining AISI 304 Austenitic Stainless Steel Flange. *Metals*, 9(9), 972. https://doi.org/10.3390/met9090972

[7] Sun, Y., Sun, J., Li, J., & Xiong, Q. (2014). An experimental investigation of the influence of cutting parameters on cutting temperature in milling Ti6Al4V by applying semi-artificial thermocouple. *The International Journal of Advanced Manufacturing Technology*, *70*, 765-773. https://doi.org/10.1007/s00170-013-5294-1

[8] Korkut, I., Kasap, M., Ciftci, I., & Seker, U. (2004). Determination of optimum cutting parameters during machining of AISI 304 austenitic stainless steel. *Materials & Design*, *25*(4), 303-305. https://doi.org/10.1016/j.matdes.2003.10.011

[9] Liew, P. J., Shaaroni, A., Razak, J., Kasim, M. S., & Sulaiman, M. A. (2017). Optimization of cutting condition in the turning of AISI D2 steel by using carbon nanofiber nanofluid. *International Journal of Applied Engineering Research*, *12*(10), 2243-2252.

[10] Sneddon, S., Xu, Y., Dixon, M., Rugg, D., Li, P., & Mulvihill, D. M. (2021). Sensitivity of material failure to surface roughness: A study on titanium alloys Ti64 and Ti407. *Materials & Design*, *200*, 109438. https://doi.org/10.1016/j.matdes.2020.109438

[11] Bouzid, L., Berkani, S., Yallese, M., Girardin, F., & Mabrouki, T. (2018). Estimation and optimization of flank wear and tool lifespan in finish turning of AISI 304 stainless steel using desirability function approach. *International Journal of Industrial Engineering Computations*, *9*(3), 349-368. https://doi.org/10.5267/j.ijiec.2017.8.002

[12] Trabelsi, S., Morel, A., Germain, G., & Bouaziz, Z. (2017). Tool wear and cutting forces under cryogenic machining of titanium alloy (Ti17). *The International Journal of Advanced Manufacturing Technology*, *91*, 1493-1505. https://doi.org/10.1007/s00170-016-9841-4

[13] Azam, M., Jahanzaib, M., Wasim, A., & Hussain, S. (2015). Surface roughness modeling using RSM for HSLA steel by coated carbide tools. *The International Journal of Advanced Manufacturing Technology*, *78*, 1031-1041. https://doi.org/10.1007/s00170-014-6707-5

[14] Peng, Z., Zhang, X., Liu, L., Xu, G., Wang, G., & Zhao, M. (2023). Effect of high-speed ultrasonic vibration cutting on the microstructure, surface integrity, and wear behavior of titanium alloy. *Journal of Materials Research and Technology*, *24*, 3870-3888. https://doi.org/10.1016/j.jmrt.2023.04.036

[15] Benardos, P. G., & Vosniakos, G. C. (2003). Predicting surface roughness in machining: a review. *International journal of machine tools and manufacture*, *43*(8), 833-844. https://doi.org/10.1016/S0890-6955(03)00059-2

[16] Seikh, A. H., Mandal, B. B., Sarkar, A., Baig, M., Alharthi, N., & Alzahrani, B. (2019). Application of response surface methodology for prediction and modeling of surface roughness in ball end milling of OFHC copper. *International Journal of Mechanical and Materials Engineering*, *14*(1), 1-11. https://doi.org/10.1186/s40712-019-0099-0

[17] Abbasi, S. A., Feng, P., Ma, Y., Zhang, J., Yu, D., & Wu, Z. (2016). Influence of microstructure and hardness on machinability of heat-treated titanium alloy Ti6Al4V in end milling with polycrystalline diamond tools. *The International Journal of Advanced Manufacturing Technology*, *86*, 1393-1405. https://doi.org/10.1007/s00170-015-8245-1

[18] Wu, J. B., Li, L., & Wang, P. J. (2024). Effect of stress relaxation on the sealing performance of O-rings in deep-sea hydraulic systems: A numerical investigation. *Engineering Science and Technology, an International Journal*, *51*, 101654. https://doi.org/10.1016/j.jestch.2024.101654

[19] Repplinger, C., Sellen, S., Kedziora, S., Zürbes, A., & Maas, S. (2024). Material modeling for numerical simulation of elastomer O-rings with experimental verification at low temperatures. *International Journal of Hydrogen Energy*, *80*, 1046-1061. https://doi.org/10.1016/j.jestch.2024.101654

[20] Oberg, E. (2016). CM; Jones, F.; Horton, H.; Ryffel, H. *Machinery's Handbook,* 30th Addition.

[21] *Parker O-Ring Handbook*. (50th Anniversary Edition). Cleveland, OH.

[22] Kashyap, V., & Ramkumar, P. (2019). Feasibility study of micro-groove cross hatched surface texturing on Ti6Al4V for improved biotribological performance in metal-on-polymer hip implant. *Tribology-Materials, Surfaces & Interfaces*, *13*(3), 150-160. https://doi.org/10.1080/17515831.2019.1606582

[23] Khanna, N., & Davim, J. P. (2015). Design-of-experiments application in machining titanium alloys for aerospace structural components. *Measurement*, *61*, 280-290. https://doi.org/10.1016/j.measurement.2014.10.059

[24] Ding, Y., Kong, L., Lei, W., Li, Q., Ding, K., & He, Y. (2024). Study on the technology of surface strengthening Ti6Al4V alloy by near-dry multi-flow channel electrode electrical discharge machining. *Journal of Materials Research and Technology*, *28*, 2219-2234. https://doi.org/10.1016/j.jmrt.2023.12.133

[25] Coromant, S. (2011). Turning tools-Main catalogue. *SandvikCoromant, Sweden*.

[26] Mitutoyo America Corporation,2016, portable surface roughness tester, surftest sj-210 series [brochure]

[27] Montgomery, D. C. (2017). *Design and analysis of experiments*. John wiley & sons. Hoboken, New Jersey

[28] Anderson, M. J., & Whitcomb, P. J. (2016). *RSM simplified: optimizing processes using response surface methods for design of experiments*. Productivity press, New York.

[29] Suresh, R., Basavarajappa, S., Gaitonde, V. N., & Samuel, G. L. (2012). Machinability investigations on hardened AISI 4340 steel using coated carbide insert. *International Journal of Refractory Metals and Hard Materials*, *33*, 75-86. https://doi.org/10.1016/j.ijrmhm.2012.02.019

Submitted: 28.09.2024

Accepted: 20.03.2025

Muhammad Azam, Research Scholar*
Prof. Dr. Mirza Jahanzaib
Department of Industrial Engineering,
University of Engineering and Technology
Taxila, Punjab, Pakistan
*Corresponding author:
Aazam1916@outlook.com